

On-Line Monitoring to Detect Sensor and Process Degradation under Normal Operational Transients

Samuel Boring and Jamie Coble

Department of Nuclear Engineering

University of Tennessee

1004 Estabrook Dr.

sboring5@vols.utk.edu; jcoble1@utk.edu

ABSTRACT

Calibration assessment of nuclear plant sensors and transmitters is currently performed through periodic maintenance actions during plant refueling outages. On-line monitoring (OLM) can be used to reduce the time and cost of this maintenance process by using empirical models to evaluate sensor calibration. The implementation of OLM can also mitigate human error associated with unnecessary maintenance on sensors operating within calibration tolerances. OLM has been studied and validated for plants under steady-state baseload operation, but the extension to load-following operation is not well-documented in the literature. Auto-associative kernel regression (AAKR) provides an error-corrected prediction of process sensor measurements for OLM through a weighted average of historic data. The current study evaluates the performance of AAKR for prediction under normal operational transients (such as expected under load-following operation). Performance of the AAKR model with two anomaly detection routines, error uncertainty limit monitoring (EULM) and sequential probability ratio test (SPRT), was evaluated for normal operation, sensor faults, and process degradation. The data used to develop and evaluate the OLM system were collected from a forced flow loop with temperature and flow sensors. Three models of well-correlated groups of sensors are trained to predict normal system behavior under planned transients. The anomaly detection routines are tested for sensor faults and process faults. The results of this experimental study suggest AAKR and an appropriate anomaly detection routine can be applied for sensor calibration and process fault detection under transient operation.

Key Words: Autoassociative Kernel Regression (AAKR), Sequential Probability Ratio Test (SPRT), Transient Operation

1 INTRODUCTION

Monitoring and control of nuclear power plants (NPPs) relies on accurate and reliable indications of key process values from plant sensors and transmitters. The current approach to ensuring measurement accuracy involves periodic calibration assessment and recalibration during refueling outages. However, unnecessary maintenance is performed under this approach, because only 5-10% of sensors undergo a drift according to a study done by the Electric Power Research Institute [1]; this periodic maintenance creates more opportunities for human error in the maintenance process, as well as making the process more costly and time consuming. NPPs can mitigate errors that occur during the maintenance process, while saving time and money, by integrating an on-line monitoring (OLM) system to detect and diagnose maintenance issues, such as sensor drift, while the plant is operating. This supports targeted maintenance actions where they are needed, instead of blanket periodic inspection and maintenance across all sensor systems. OLM has been well studied for various applications in NPPs over the last several decades, but OLM has not been widely implemented commercially in NPPs due to existing technical gaps and uncertainties [2].

The OLM system for calibration assessment consists of a system model and an anomaly detection routine. For the current research, auto-associative kernel regression (AAKR) is implemented as an error correction routine that estimates the expected sensor measurements based on redundant and related sensor values. Two anomaly detection routines are investigated that have commonly been used for calibration assessment: simple signal thresholding (SST) and the sequential probability ratio test (SPRT). These prediction and detection methodologies are described in greater detail in Section 2. Section 3 presents the experimental testbed used to collect data to test the proposed OLM system.

The results of these tests are given in Section 4. Section 5 summarizes the work and highlights areas of ongoing research.

2 METHODOLOGY

The OLM system investigated here consists of a prediction model (AAKR) and an anomaly detection routine (SST or SPRT). These methodologies are discussed in the following subsections.

2.1 Auto-Associative Kernel Regression

Auto-associative kernel regression (AAKR) is a non-parametric, memory-based modeling technique that uses a matrix of historic memory vectors, X_m ($n \times p$), to calculate a weighted average to predict the expected measurement vector, \hat{x}_q ($1 \times p$), given a query vector, x_q ($1 \times p$). First, the distance between the query vector, x_q , and each memory vector, m_i , is calculated. This is typically done using a Euclidean distance, though other distance metrics have been proposed [3]:

$$d_i = \sqrt{\sum_{j=1}^p (x_{q,j} - x_{m,i,j})^2}. \quad (1)$$

This distance is then converted to a weight using a kernel function, such as the Gaussian kernel with bandwidth h :

$$w_i = e^{-\frac{d_i^2}{h^2}}. \quad (2)$$

Finally, the predicted query vector is found as a weighted average of the memory vectors:

$$\hat{x}_q = \frac{\sum_{i=1}^n w_i m_i}{\sum_{i=1}^n w_i}. \quad (3)$$

Because AAKR estimates the expected value of the entire measurement (query vector), it can be thought of as an error-correction routine. AAKR relies on the relationships between variables to make predictions about their true values. For this reason, inputs to the kernel regression model must be well-correlated to each other. Sensors are grouped together based on their linear inter-correlation; this is done by calculating the Pearson correlation coefficient for each sensor with respect to every other sensor. Correlation coefficients show the linear dependence of one sensor to another sensor. Groups of sensors are identified based on a cutoff magnitude of the correlation coefficients. After the groups are identified, an AAKR model is trained for each group.

2.1.1 Model Training

The training data are stored in a memory matrix, but model runtime can be decreased and accuracy improved by keeping a well-selected subset of training data as memory vectors. Three memory vector selection methods are considered in this project: max-min, sort-select, and combination-selection methods [4]. The max-min method selects vectors based on local maximum and minimum value for each sensor. The sort-select method sorts the data according to the magnitude of each observation and periodically samples from the sorted list. The combination-selection method uses a combination of the max-min and sort-select methods, starting by selecting observations containing the minimum and maximum values for each signal and then selecting remaining observations using the sort-select approach.

2.1.2 Model Optimization

The optimization process uses an independent test data set to evaluate different models with specified variables: number of memory vectors, vector selection method, and kernel bandwidth. The optimization procedure applies a brute-force search of the combination of provided values for each of the three model parameters. The models are compared using the mean squared error (MSE), shown in (4).

$$e_j = \frac{1}{n_t} \sum_{k=1}^{n_t} [\hat{x}_{k,j} - x_{k,j}]^2 \quad (4)$$

where $\hat{x}_{k,j}$ is the k^{th} prediction of the j^{th} sensor, $x_{k,j}$ is the k^{th} measurement of the j^{th} sensor, and n_t is the number of observations in the test data set.

2.1.3 Performance Characterization

A third independent set of nominal data, validation data, is used to evaluate the model performance in terms of several performance characteristics, such as accuracy, auto- and cross-sensitivity, uncertainty, and fault detectability [4]; the current research primarily focuses on accuracy and auto- and cross-sensitivity. Accuracy characterizes the model's prediction performance on fault-free data; this is evaluated through the root mean square error (RMSE):

$$\text{Acc}_i = \sqrt{\frac{\sum_{j=1}^{n_v} (\hat{x}_{j,i} - x_{j,i})^2}{n_v}} \quad (5)$$

where $\hat{x}_{j,i}$ is the model prediction of the i^{th} variable of the j^{th} observation and n_v is the number of observations in the validation data set. Auto-sensitivity characterizes the effect of an error in an input signal on the error-corrected prediction of that signal:

$$\text{AS}_i = \frac{\|\hat{x}_i^d - \hat{x}_i\|}{\|x_i^d - x_i\|} \quad (6)$$

where x_i^d is the drifted (or otherwise faulted) version of the true measurement of the i^{th} sensor, x_i ; \hat{x}_i^d is the model prediction of the drifted input; and \hat{x}_i is the model prediction of the undrifted input. Similarly, cross-sensitivity measures the magnitude of the effect of an error in an input signal on the prediction of a different output signal:

$$\text{CS}_i = \frac{\|\hat{x}_i^d - \hat{x}_i\|}{\|x_k^d - x_k\|} \quad (7)$$

where x_k^d is a drifted version of the true measurement of the k^{th} sensor, x_k . These three metrics together give a view of the model performance with nominal, unfaulted inputs (accuracy) and faulted inputs (auto- and cross-sensitivity). In every case, these metrics should be as small as possible to provide accurate and robust predictions under all possible scenarios. Comparisons of the measured data and model predictions, called residuals, are used in three anomaly detection methods to determine if any faults have occurred.

2.2 Anomaly Detection Methods

This project compares two anomaly detection methods: simple signal thresholding (SST) and sequential probability ratio test (SPRT). The SST method detects an anomaly if a residual surpasses a threshold. Thresholds for this project are determined based on the residuals of the validation data. By placing thresholds on model residuals instead of directly on signal values, subtle changes in the relationships between signals can be detected, resulting in a faster detection than relying on gross changes in a single sensor value.

The SPRT method is a statistical hypothesis test that evaluates the ratio of the likelihood that a series of residuals result from a nominal distribution or from a faulted distribution [5]. The test statistic at the i^{th} observation, S_i , for this hypothesis test is a running sum of the log-likelihood ratio, given by:

$$S_i = S_{i-1} + \log(\Lambda_i) \quad (8)$$

where S_{i-1} is the test statistic from the previous observation and Λ_i is the likelihood ratio. When the nominal and faulted distributions are assumed to be Gaussian distributions with equal variance and offset means, the likelihood ratio is:

$$\Lambda_i = e^{-\left[\frac{(r_i - \mu_o)^2 - (r_i - \mu_1)^2}{2\sigma^2}\right]} \quad (9)$$

where r_i is the residual of the i^{th} observation, μ_o is the mean of the nominal distribution, μ_1 is the mean of the faulted (alternative) distribution, and σ^2 is the common variance of both the nominal and faulted distributions. At each observation, the test statistic is updated and compared to two thresholds to determine if (a) the null hypothesis must be accepted (i.e., there is no fault), (b) the alternative hypothesis must be accepted (i.e., there is a fault), or (c) a decision cannot be made. In either case (a) or (b), the test statistic is reset to $S_i = 0$ and monitoring continues. If a decision cannot be made, the system continues to monitor.

The thresholds for the SPRT method are calculated using the desired false alarm (α) and missed alarm (β) probabilities, which are set to 0.1 and 0.01, respectively. Two threshold are calculated:

$$A = \ln \frac{\beta}{1-\alpha} \quad (10)$$

$$B = \ln \frac{1-\beta}{\alpha} \quad (11)$$

If the test statistic is greater than B a fault is detected (the alternative hypothesis is accepted); if the test statistic is less than A there is no evidence of a fault (the null hypothesis is accepted). If the test statistic is in between A and B the state of the observation is unknown, though for the purposes of OLM, the null hypothesis (no fault) is assumed true until proven otherwise.

3 EXPERIMENTAL TESTBED

3.1 Flow Loop

Data are collected from a forced flow loop are used to develop and evaluate the proposed OLM system. Figure 1 gives a schematic of the two loop system with sensors and major components indicated. The primary loop features an adjustable 9 kW heater, variable speed pump, redundant flow meters (magnetic flow meter and Coriolis flow meter), and temperature sensors at the inlet and outlet of the heater and inlet and outlet of heat exchanger. Two additional redundant temperature sensors not indicated on the diagram, labeled FRTD1 and FRTD2, are located between the pump outlet and the heater inlet. The secondary loop has a motor operated valve to control coolant flow from the building water supply as well as temperature sensors before and after the heat exchanger and a magnetic flow meter (not shown). Two additional valves are included to simulate process disturbances: a bypass valve diverts flow on the secondary side of the heat exchanger, effectively reducing heat exchanger efficiency, and a throttle valve at the output of the primary loop pump simulates pump degradation or increased flow resistance.

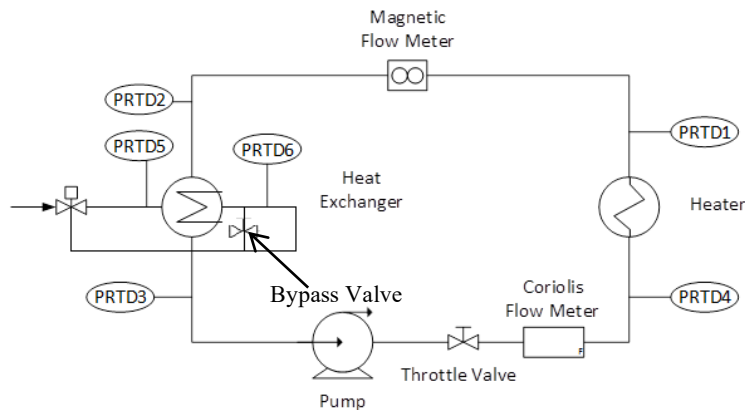


Figure 1. Setup of the sensors and valves on the flow loop

The loop is operated under normal transient conditions, with the heater power varied in a step-ramp between 50 and 100% power; a typical ramp is shown in Figure 2. The primary and secondary flow rates are controlled with proportional-integral (PI) controllers to maintain temperature setpoints at the inlet and outlet of the heater. Details of the flow loop operation and control are given in [6]. In addition to nominal operation data, process faults are simulated using the bypass and throttle valves. First, flow restriction (either due to increased flow resistance or pump degradation) is simulated by slowly closing the throttle valve at the primary pump outlet with each run of the heater load profile; this is referred to as the throttle valve data in the remainder of the paper. Heat exchanger fouling is simulated by gradually opening the bypass valve on the secondary loop; this is called the bypass data. These two process faults are investigated independently; no simulation of both faults occurring simultaneously has been considered yet. Finally, sensor faults are numerically simulated post data collection by adding a small drift to one process sensor, called the sensor drift data. Control sensor faults have not been studied here and are an area of future work.

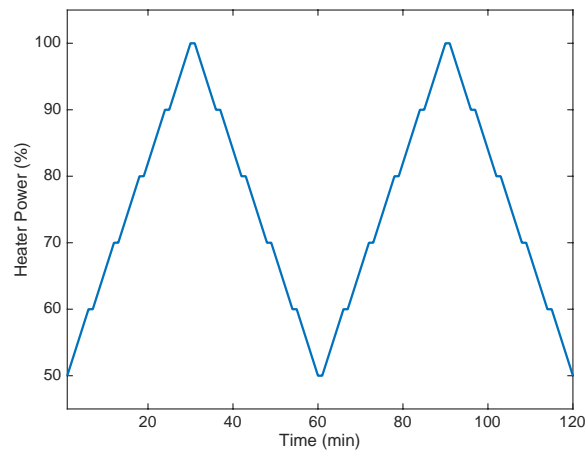


Figure 2. Example heater ramp from 50-100% power. Heater power is incremented 10% over 3 minutes, then held constant for 2 minutes before moving to the next power ramp.

3.1.1 Data Complications

The nominal fault-free data are the data collected when the throttle valve is fully open and the bypass valve is completely closed. For both fault conditions, fault-free data are collected before the fault condition is applied. A problem arose when selecting the training, test, and validation data for developing the OLM model: the maximum of the throttle valve data is outside of the bounds of the bypass data and the minimum of the bypass data is outside the bounds of the throttle valve data, this can be seen in Figure 3. This is a concern because an AAKR model can only generate prediction values that are in the bounds of its memory matrix. This is solved by using the bypass data with the second half of the valve data; this ensures that all of the fault-free data are within the bounds of the data used to create the model.

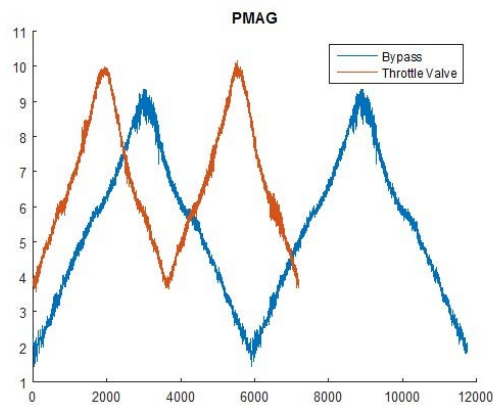


Figure 3. Comparison of the bypass and throttle valve data sets.

4 RESULTS

The training data are used to divide the measured data into correlated subgroups. Three groups are identified: group 1 includes the primary magnetic flow meter (PMAG), the primary Coriolis meter (Cor), the secondary magnetic flow meter (SMAG), and the heater inlet temperature sensor (PRTD4); group 2 includes the heater outlet temperature (PRTD1), the primary side heat exchanger inlet and outlet (PRTD2 and PRTD3, respectively), and the redundant temperature sensors prior to the heater inlet (FRTD1 and FRTD2); and group 3 includes the primary magnetic flow

meter (PMAG), the primary Coriolis meter (Cor), the primary side heat exchanger inlet (PRTD2) and the secondary side heat exchanger outlet (PRTD6). The secondary side heat exchanger inlet temperature (PRTD5) was largely constant, as that temperature is dictated by the building supply system, and was not sufficiently correlated with anything to include in a model group. Three AAKR models were developed to monitor the three groups of sensors under simulated process and sensor fault conditions. The SST and SPRT anomaly detection routines were applied to faulted system results to evaluate detectability. These results are presented below.

4.1 Anomaly Detection

The proposed OLM system monitors each sensor included in at least one model for indications of fault conditions. A subset of those results is presented here to highlight sensors that potentially indicate the simulated process and sensor faults. Two examples are presented here: the bypass process fault and the sensor drift.

4.1.1 Bypass Process Fault

Opening the heat exchanger bypass valve effectively reduces the heat exchanger efficiency, so that the outlet temperature of the secondary side coolant is lower than would be expected under normal conditions. Figure 4 shows the OLM system results for the secondary side outlet temperature (PRTD6 in Figure 1); these results come from the group 3 model given above. The top plot shows the OLM system residuals for the heat exchanger outlet temperature. The red lines indicate the SST thresholds, while the vertical line shows the onset of the degradation (bypass valve opening). The second plot shows the results of SST fault detection; this approach shows very few false alarms, but does not detect the degradation until well into the onset of fault. The bottom plot shows the SPRT results; here, there are several spurious alarms during the nominal operation period, but the reliable fault detection occurs earlier in the fault progression. The spurious alarms could potentially be filtered through a logical fault consolidation [7]; this is being investigated currently.

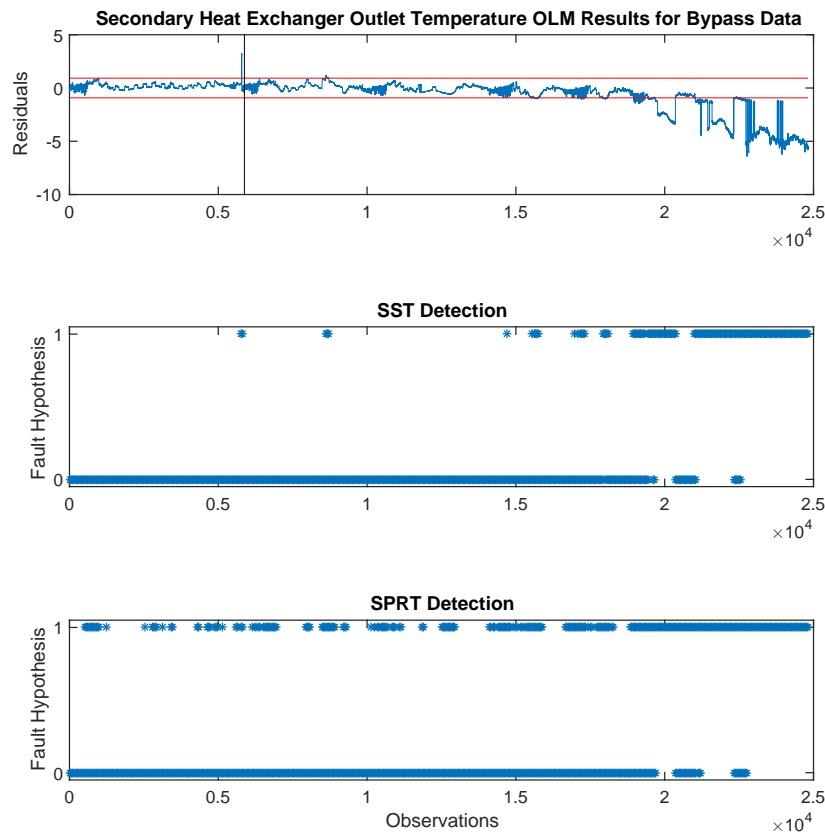


Figure 4. OLM system results for the secondary side heat exchanger outlet under simulated heat exchanger fouling.

4.1.2 Sensor Drift Fault

Process sensor drift was simulated by numerically adding a drift to nominal process data. The simulated drift began at the 2000th observation and was introduced into the primary loop magnetic flow meter. The results of the OLM detection system are shown in Figure 5. The top plot shows the model residuals for the primary side magnetic flow meter resulting from the group 1 model. Again, the SST thresholds are indicated as well as the onset of the fault. In this case, the SST results (shown in the middle plot) detect the fault quickly and reliably. The SPRT approach, shown in the bottom plot, results in a significant number of false alarms prior to fault onset. This may indicate that the distributions of faulted and unfaulted data are not appropriate; this is being investigated.

Figure 6 illustrates the concerns with model cross-sensitivity. The figure shows the prediction residuals for all four signals in the AAKR model. The heater inlet temperature signal is robust to the faulted input in the primary magnetic flow meter, but the other flow meters are not. In this case, a fault detection routine would likely indicate faults in all three flow signals. This leads to the need for a robust diagnostic algorithm to isolate the root cause of the alarms. Fault diagnosis is an area of ongoing research, investigating methods to isolate all the simulated fault modes considered, including process faults and sensor faults in several process sensors.

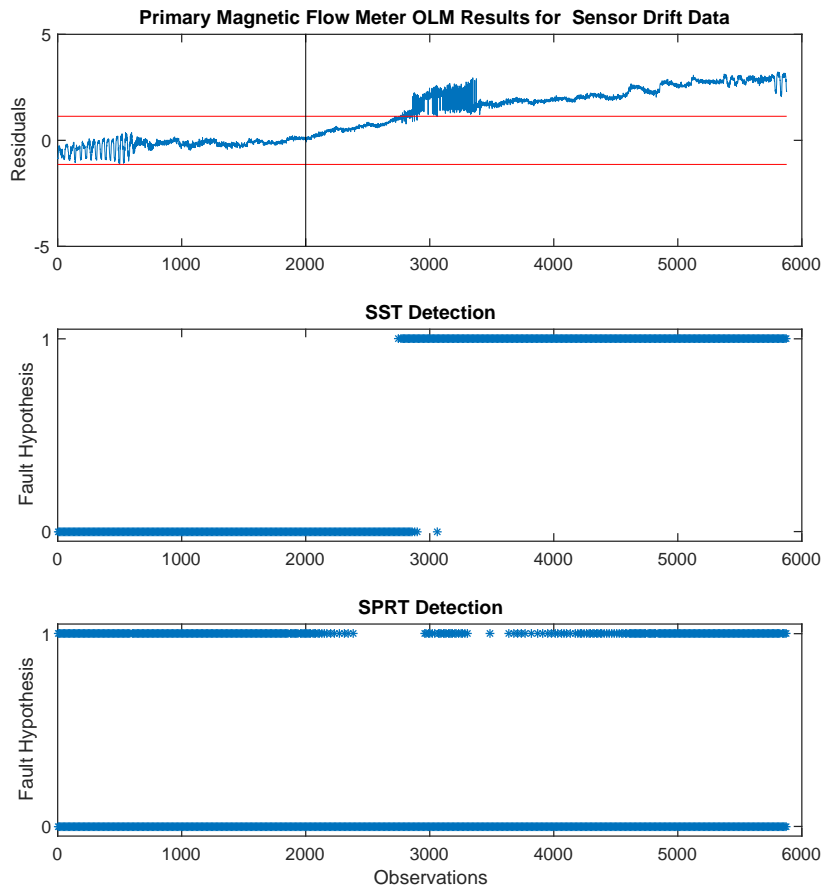


Figure 5. OLM system results for the primary loop magnetic flow meter under simulated sensor drift.

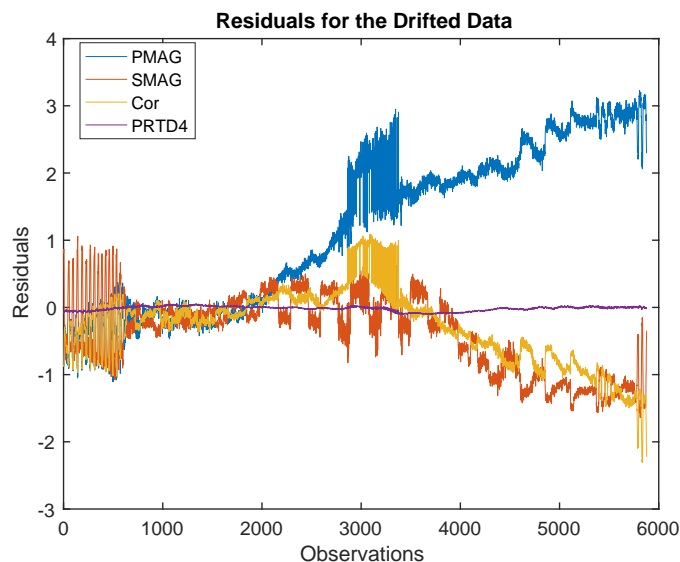


Figure 6. Residuals of all four signals in group 1 model under simulated drift of the primary side magnetic flow meter (PMAG). Significant spillover can be seen in the primary side Coriolis measurement (Cor) and the secondary side magnetic flow meter (SMAG).

5 ONGOING WORK

Several areas of ongoing work have been highlighted: investigation of control sensor faults that are subject to control sensor masking; optimization of SPRT nominal and faulted distributions for robust detection across all fault modes; and fault diagnosis to isolate the root cause of faults. If a sensor fault has been detected and identified, the fault could potentially be mitigated temporarily through a so-called virtual sensor: an estimate of the true sensor value. This would allow a facility to continue to operate under limited sensor failures until a convenient maintenance period, such as a refueling outage, instead of requiring an immediate action to repair or replace the damaged sensor.

6 CONCLUSIONS

The current approach to sensor calibration assessment is time-intensive and expensive; it negatively impacts the economics of plant operations, and research and operating history both suggest that sensors can reliably operate over much longer periods of time within required calibration specifications. The research described here attempts to address some of the technical gaps in applying OLM for sensor calibration assessment to load-following reactors. The results of this preliminary study suggest that the previously developed approaches to online calibration assessment will be applicable to facilities operating under normal transient loads. Several areas remain to fully develop this approach, including considering additional faults and anomalies, optimizing the anomaly detection routines, and developing fault diagnostic algorithms.

ACKNOWLEDGMENTS

The work presented here was funded by the US Department of Energy Office of Nuclear Energy (DOE-NE) Nuclear Energy Enabling Technology Advanced Sensors and Instrumentation (NEET-ASI) program.

REFERENCES

1. EPRI, *On-line Monitoring of Instrument Channel Performance: TR-104965-R1 NRC SER*. 2000: Palo Alto, CA.
2. Coble, J.B., et al., *A Review of Sensor Calibration Monitoring for Calibration Interval Extension in Nuclear Power Plants*. 2012: Pacific Northwest National Laboratory.

3. Garvey, D. and J. Hines, *Robust Distance Measures for On-Line Monitoring: Why Use Euclidean?*, in *Applied Artificial Intelligence*. 2006, World Scientific. p. 922-929.
4. Hines, J.W., et al., *Technical Review of On-line Monitoring Techniques for Performance Assessment, Volume 2: Theoretical Issues*. 2008, U.S. Nuclear Regulatory Commission: Washington, D.C.
5. Wald, A., *Sequential Tests of Statistical Hypotheses*. *Annals of Mathematical Statistics*, 1945. **16**(2): p. 117-186.
6. Coble, J., R. Tarver, and J.W. Hines, *Calorimetric Analysis to Infer Primary Circuit Flow in Integral and Pool-Type Reactors*. *IEEE Transactions on Nuclear Science*, 2017. **64**(2): p. 837-843.
7. Hines, J., et al., *Technical Review of On-line Monitoring Techniques for Performance Assessment, Volume 3: Limiting Case Studies*. Technical review NUREG/CR-6895, 2008. **3**: p. 20555-0001.